1-1-2015

3D-mesa 'bridge' silicon microdosimeter: charge collection study and application to RBE studies in 12C radiation therapy

Linh T. Tran
University of Wollongong

Lachlan Chartier
University of Wollongong, lc752@uowmail.edu.au

Dale A. Prokopovich
ANSTO, dalep@uow.edu.au

Mark I. Reinhard
ANSTO

Marco Petasecca
University of Wollongong, marcop@uow.edu.au

See next page for additional authors

3D-mesa 'bridge' silicon microdosimeter: charge collection study and application to RBE studies in 12C radiation therapy

Abstract

Microdosimetry is an extremely useful technique, used for dosimetry in unknown mixed radiation fields typical of space and aviation, as well as in hadron therapy. A new silicon microdosimeter with 3D sensitive volumes has been proposed to overcome the shortcomings of the conventional Tissue Equivalent Proportional Counter. In this article, the charge collection characteristics of a new 3D mesa microdosimeter were investigated using the ANSTO heavy ion microprobe utilizing 5.5 MeV rm He^{2+} and 2 MeV rm H + ions. Measurement of the microdosimetric characteristics allowed for the determination of the Relative Biological Effectiveness of the 12rm C heavy ion therapy beam at the Heavy Ion Medical Accelerator in Chiba (HIMAC), Japan. Well-defined sensitive volumes of the 3D mesa microdosimeter have been observed and the microdosimetric RBE obtained showed good agreement with the TEPC. The new 3D mesa 'bridge' microdosimeter is a step forward towards a microdosimeter with fully free-standing 3D sensitive volumes.

Disciplines

Engineering | Science and Technology Studies

Publication Details

Tran, L. T., Chartier, L., Prokopovich, D. A., Reinhard, M. I., Petasecca, M., Guatelli, S., Lerch, M. L. F., Perevertaylo, V. L., Zaider, M., Matsufuji, N., Jackson, M., Nancarrow, M. & Rosenfeld, A. B. (2015). 3D-mesa 'bridge' silicon microdosimeter: charge collection study and application to RBE studies in 12C radiation therapy. IEEE Transactions on Nuclear Science, 62 (2), 504-511.

Authors

Linh T. Tran, Lachlan Chartier, Dale A. Prokopovich, Mark I. Reinhard, Marco Petasecca, Susanna Guatelli, Michael L. F Lerch, Vladimir L. Perevertaylo, Marco Zaider, Naruhiro Matsufuji, Michael Jackson, MItchell Nancarrow, and Anatoly B. Rosenfeld

3D-Mesa "Bridge" Silicon Microdosimeter: Charge Collection Study and application to RBE Studies in ^{12}C Radiation Therapy

Linh T. Tran, *Student Member IEEE*, Lachlan Chartier, *Student Member IEEE*, Dale A. Prokopovich, Mark I. Reinhard, Marco Petasecca, *Member IEEE*, Susanna Guatelli, *Member IEEE*, Michael L. F. Lerch, *Member IEEE*, Vladimir L. Perevertaylo, Marco Zaider, Naruhiro Matsufuji, Michael Jackson, Mitchell Nancarrow and Anatoly B. Rosenfeld, *Senior Member IEEE*

***Abstract*– Microdosimetry is an extremely useful technique, used for dosimetry in unknown mixed radiation fields typical of space and aviation, as well as in hadron therapy. A new silicon microdosimeter with 3D sensitive volumes has been proposed to overcome the shortcomings of the conventional Tissue Equivalent Proportional Counter. In this article, the charge collection characteristics of a new 3D mesa microdosimeter were investigated using the ANSTO heavy ion microprobe utilizing 5.5 MeV He^{2+} and 2 MeV H^{+} ions. Measurement of the microdosimetric characteristics allowed for the determination of the Relative Biological Effectiveness of the ^{12}C heavy ion therapy beam at the Heavy Ion Medical Accelerator in Chiba (HIMAC), Japan. Well-defined sensitive volumes of the 3D mesa microdosimeter have been observed and the microdosimetric RBE obtained showed good agreement with the TEPC. The new 3D mesa "bridge" microdosimeter is a step forward towards a microdosimeter with fully free-standing 3D sensitive volumes.**

***Index Terms*—Microdosimetry, heavy ion therapy, silicon microdosimeter, 3D mesa, charge collection, IBIC.**

I. Introduction

MICRODOSIMETRY is a method of measuring the microscopic pattern of ionizing energy deposition in a micron sized sensitive volume (SV) of similar dimensions to biological cells [1]. This technique is extremely useful for dosimetry in unknown mixed radiation fields typical of space and aviation, as well as in hadron therapy. The microdosimetric quantity used to describe the energy deposition in such a volume along a particles track is called the lineal energy deposition (y).

$$y = \frac{E}{< l >}$$

where E is the energy deposited in a micron sized SV with an average chord length $<l>$. The spectrum of stochastic events $f(y)$ for all primary and secondary particles generated during an exposure of tissue to ionizing radiation can be derived from the spectrum of energy deposition events. The dose distribution $d(y)$ is given by:

$$d(y) = \frac{yf(y)}{\overline{y_F}}$$

where $\overline{y_F} = \int_0^\infty yf(y)dy$ and $\overline{y_D} = \int_0^\infty yd(y)dy$; $\overline{y_F}$ is frequency mean lineal energy and $\overline{y_D}$ is dose mean lineal energy.

Conventional detectors used for microdosimetry are tissue equivalent proportional counters (TEPC) which are advantageous due to their spherical sensitive volume and tissue equivalency through use of a tissue equivalent gas. However, TEPCs have several limitations such as high voltage operation, large size of assembly, which reduces spatial resolution and have other disadvantages such as the wall effect [2], and an inability to simulate multiple cells.

The Centre for Medical Radiation Physics (CMRP), University of Wollongong, has initiated the concept of silicon microdosimetry to address the shortcomings of the TEPC [3, 4]. Three generations of silicon on insulator (SOI) microdosimeters have been developed, fabricated and investigated [4-7]. Based on previous research and development at CMRP, the feasibility of the silicon microdosimetry concept has been proven. Despite this success, a number of limitations have been observed in previous designs of SOI microdosimeter. These limitations include non-uniformity of charge collection in the SV and diffuse charge collection outside of the SV [6]. In order to overcome these drawbacks, we have proposed further steps to optimize the SOI microdosimeters with the development of freestanding 3D

L. T. Tran, L. Chartier, S. Guatelli, M. Petasecca, M. L. F. Lerch and A. B. Rosenfeld are with the Centre for Medical Radiation Physics, University of Wollongong, NSW 2522, Australia (e-mail: tlt822@uowmail.edu.au; lc52@uowmail.edu.au; susanna@uow.edu.au; marcop@uow.edu.au, mlerch@uow.edu.au; anatoly@uow.edu.au).

D. A. Prokopovich and M. I. Reinhard are with the Institute of Materials Engineering, Australian Nuclear Science and Technology Organisation, Lucas Heights, NSW2234, Australia (e-mail: dpr@ansto.gov.au; mrz@ansto.gov.au).

V. L. Perevertaylo is with SPA-BIT, Kiev, Ukraine.

M. Zaider is with the Department of Medical Physics, Memorial Sloan-Kettering Cancer Center, New York, NY 10065 USA (email: zaiderm@mskcc.org).

N. Matsufuji is with Research Centre for Charge Particle Therapy, National Institute of Radiological Science, Japan. (email: matufuji@nirs.go.jp).

M. Jackson is with the University of New South Wales, Sydney NSW 2052, Australia. (email: michael.jackson@sesiahs.health.nsw.gov.au)

M. Nancarrow is with Electron Microscopy Centre, University of Wollongong, Wollongong, New South Wales 2500, Australia. (email: nancarro@uow.edu.au)

SVs, the so called "mushroom" microdosimeter, using 3D detector technology [8]. A Geant4 simulation study has been carried out to optimize the design and investigate the response of the "mushroom" microdosimeter in aviation neutron fields. These results have given confidence to the new microdosimeter design [9]. However, the manufacturing process for fabricating free-standing 3D SVs on a silicon substrate is complex. As an intermediate step towards free-standing 3D SVs, an SOI microdosimeter with 3D mesa SVs was produced by etching the silicon surrounding the SVs whilst leaving thin silicon "bridges" between the SVs to support the aluminum tracks. Mesa structures have been implemented previously in the second generation CMRP microdosimeter [10]. However, a low yield of SVs has been observed due to damage of the Al tracks lifted over the steep 10 µm mesa structure of each SV. The new microdosimeter is called the "bridge" microdosimeter as it has thin Si bridges connecting the SVs. The charge collection study of the new device and its application for RBE determination in ^{12}C radiation therapy is presented.

II. Material and Method

A. Design of the 3D mesa bridge microdosimeter detectors

The newly developed bridge microdosimeter has a large sensitive area of 4.1 x 3.6 mm^2 designed for use in low dose rate environments such as those in aviation and space. The device is segmented into three sections in order to reduce the noise by minimizing the capacitance and reverse current of each segment. The microdosimeter is based on an array of planar 30 x 30 x 10 µm cubic SVs fabricated on a high resistivity of 3 kΩ.cm n-SOI active layer of thickness 10 µm and low resistivity supporting wafer. Layers of phosphorus silicate glass (PSG) and SiO_2 were deposited on top of the device. Each SV was fabricated using ion implantation to produce the square p-n junction structure. The 10 µm thick mesa structure of each SV was produced using an ion plasma etching process. The even and odd rows of SVs are read out independently to avoid events in adjacent sensitive volumes being read as a single event in the case of oblique charged particle tracks.

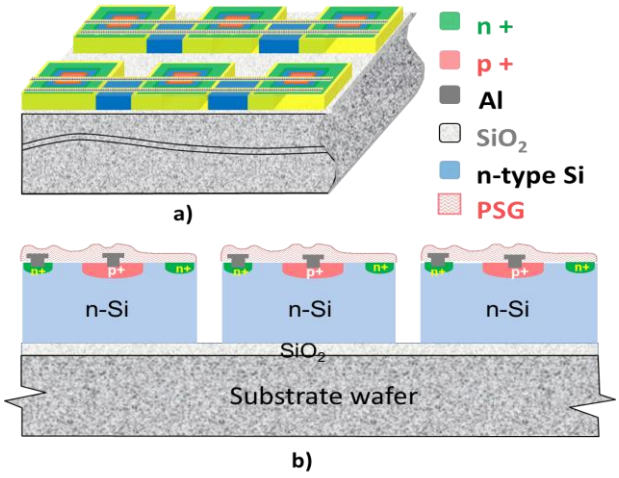

Fig. 1. Schematic of the design of SOI bridge microdosimeter. (a) 3D view. (b) A cross-section of the microdosimeter behind the silicon bridge.

Fig. 1 shows a simplified section of the 3D mesa bridge microdosimeter designed to provide well-defined 3D SVs as well as eliminate charge sharing between neighboring SVs.

B. Scanning Electron Microscopy Study

The structure of the "bridge" microdosimeter was studied using a Japan Electron Optics Laboratory (JEOL) Scanning Electron Microscope (SEM) at the Australian Institute for Innovative Materials (AIIM), University of Wollongong. The SEM is capable of producing 3D images with resolution of approximately 2 nm.

C. Ion Beam Induced Charge Collection (IBICC) Technique

The charge collection efficiency for the 3D mesa bridge microdosimeter was investigated using the IBICC technique with the Australian National Tandem for Applied Research (ANTARES) heavy ion microprobe at Australian Nuclear Science and Technology Organisation (ANSTO) [11]. A monoenergetic beam of ions focused to a diameter of approximately 1 µm was raster scanned over the surface of the microdosimeter. The ions and their energies used in this study are shown in Table 1. The linear energy transfer (LET) values of the ions were taken from SRIM 2008. The IBICC signal corresponding to the beam position (X, Y) as well as the charge collection E for each event was processed into an event-by-event list mode file. Median energy maps showing the charge collection characteristics of the device were then created. Energy calibration of the spectroscopy chain was performed using a pulse generator which was calibrated with a 300 µm thick planar silicon PIN diode with 100% Charge Collection Efficiency (CCE) exposed to the ion sources used in the IBICC experiment.

TABLE I

CHARACTERISTICS OF IONS USED IN THE IBICC STUDY

Ion	Energy (MeV)	Entrance LET in Si (keV/µm)	Range in Si (µm)
^{1}H	2.0	26.09	47.69
^{4}He	5.5	133.4	28.02

D. Experiment at ^{12}C ion therapy facility - Heavy Ion Medical Accelerator in Chiba (HIMAC), Japan

The 3D mesa bridge microdosimeter was placed in various positions along the central axis of the Spread Out Bragg Peak (SOBP) of a 290 MeV/u ^{12}C ion beam at the Heavy Ion Medical Accelerator in Chiba (HIMAC), Japan. A modular polymethyl methacrylate (PMMA) phantom was used to adjust the position of the Bragg peak relative to the device.

The Relative Biological Effectiveness (RBE_{10}) of the ^{12}C ion beam is defined as the ratio of the dose required to achieve 10% cell survival using X-rays to that required when using the radiation of interest.

The modified microdosimetric-kinetic model (MKM) [13] relates the microdosimetric parameter known as the dose-mean lineal energy $\overline{y_d}$ to the Linear Quadratic Model (LQM) parameter α, for a particular radiation field. The relation between α and $\overline{y_d}$ is presented in equation (3) where $\overline{y_d}$ is replaced by y* (4), the saturation-corrected dose-mean lineal energy, used in the case of excessive local energy deposition

which leads to the over-killing effect (saturation effect). Hence, it is possible to derive the RBE_{10} from experimentally measured microdosimetric spectra.

Using the LQM of the cell survival response to radiation S in equation (1), the RBE_{10} can be expressed as in equation (2) [15]:

$$S = \exp[-\alpha D - \beta D^2] \quad (1)$$

$$RBE_{10} = \frac{2\beta D_{10,R}}{\sqrt{\alpha^2 - 4\beta ln(0.1)} - \alpha} \quad (2)$$

where α, β are tissue radio-sensitivity coefficients (α, in units of Gy^{-1} and β, in units of Gy^{-2}). $D_{10,R}$ = 5.0 Gy is the 10% survival dose for human salivary gland (HSG) tumor cells using 200 kVp X-rays

$$\alpha = \alpha_o + \frac{\beta}{\rho \pi r_d^2} y^* \quad (3)$$

where $\alpha_0 = 0.13\ Gy^{-1}$ is a constant that represents the initial slope of the survival fraction curve in the limit of zero LET, $\beta = 0.05\ Gy^{-2}$ is a constant independent of LET, $\rho = 1\ g/cm^3$ is the density of tissue and $r_d = 0.42\ \mu m$ is the radius of a sub-cellular domain in the MK model.

$$y^* = \frac{y_o^2 \int_0^\infty (1 - exp(-y^2/y_o^2)) f(y) dy}{\int_0^\infty y f(y)\, dy} \quad (4)$$

y_o = 150 keV/μm is used in this study in order to match the calculation method used at HIMAC in experiments with the TEPC.

The lineal energy deposition was measured using a silicon microdosimeter and therefore a conversion factor is required to obtain the simulated lineal energy deposition in tissue equivalent material. A conversion factor of 0.63 was used as derived previously [16].

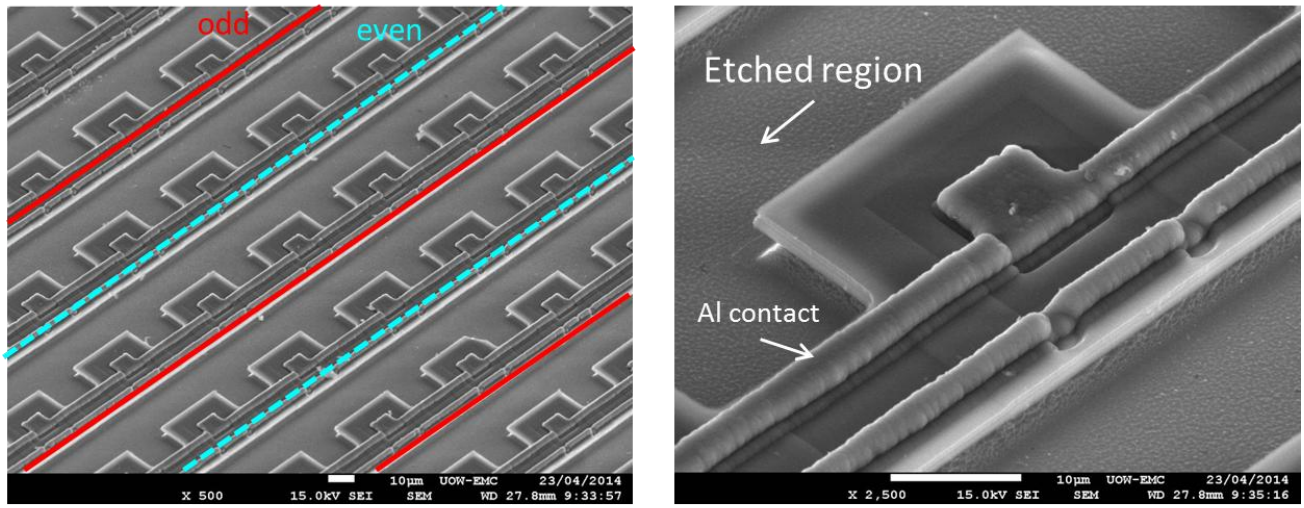

Fig. 2. SEM images of arrays of SVs. (a) Array of sensitive volumes titled at 45°. (b) Single sensitive volume.

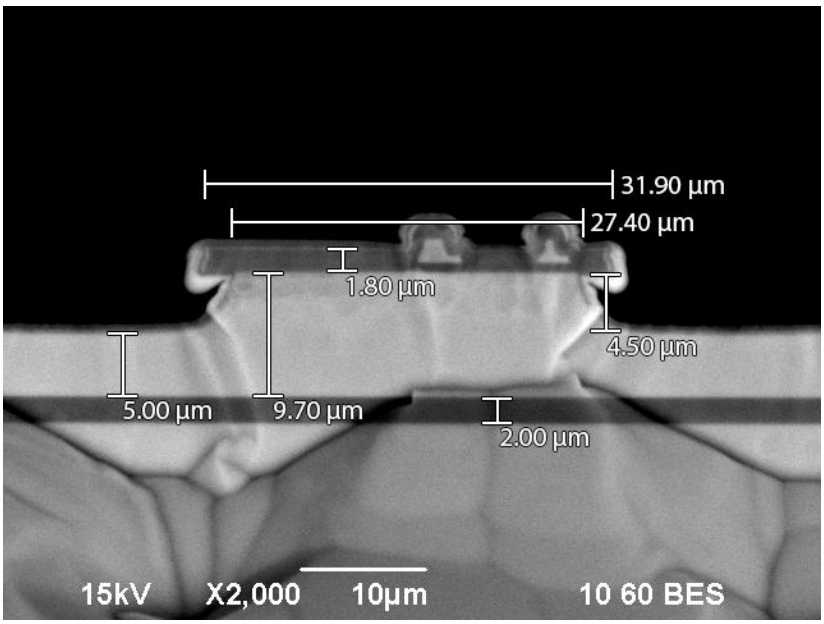

Fig. 3 Cross-section image of a single SV.

III. Results and Discussions

A. SEM Images of 3D mesa bridge microdosimeter

Fig. 2 a shows SEM image of arrays of SVs where both the etched region outside the SVs and Al tracks connecting p^+ cores and n^+ lateral regions placed on "bridges" between SVs are clearly visible.

Fig. 2 b shows magnified image of single SV. It can be seen that the 3D SV has a truncated square pyramid shape due to different etching times along the SVs depth. The top layer above the SVs (Fig. 2 b) is the SiO_2 and Phosphor Silicate Glass (PSG) layers with original size of the SV 30 µm x 30 µm which has not been etched due to selective etching.

Fig. 3 shows a SEM cross sectional image of a single SV. An oxide layer 2 µm in thickness can be clearly seen between the active region and support wafer. Silicon surrounding the SV was etched to a depth of approximately 4.5 µm, leaving a 5 µm thick layer of silicon due to incomplete etching.

B. Charge Collection Studies

a) Response of bridge microdosimeter to 2 MeV H^+ ions

The response of the bridge microdosimeter to 2 MeV H^+ ions is presented in Fig. 4. The peak of the deposited energy distribution in the 10 µm bridge microdosimeter is approximately 245 keV which is close to expected value of 270 keV from 2 MeV H^+ ions in 10 µm of silicon, calculated by SRIM 2008.

Fig. 5 shows the charge collection in the SVs of two adjacent rows of an even array at -10 V bias with the odd array also biased at -10 V however not connected to charge readout electronics. Very low energy events with less than 40 keV were observed when ions were incident outside the SVs. The energy threshold was as low as 16 keV, corresponding to around 0.7 keV/µm of lineal energy threshold in a tissue equivalent SV. No cross talk was observed between odd and even arrays. Fig. 6 shows the charge collection in a single SV at different biases. Even without bias almost 100% charge collection efficiency (CCE) under the 10 µm x 10 µm core p^+ region of the SVs was observed, while at -10 V bias the charge collection region conforms to the physical shape of the SV. In Fig. 6b, the white dashed square represents an area of 28 x 28 µm, corresponding to the edge of the n^+ region of the SV, as seen in Fig. 1.

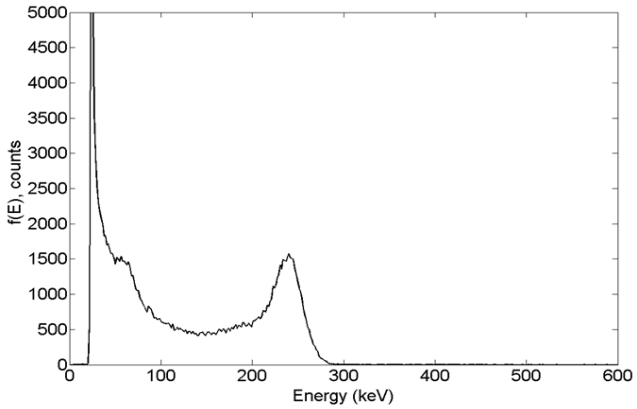

Fig. 4 Energy spectrum obtained from 10 µm thick n-SOI bridge microdosimeter irradiated with 2 MeV H^+ ions. The detector was biased at -10 V.

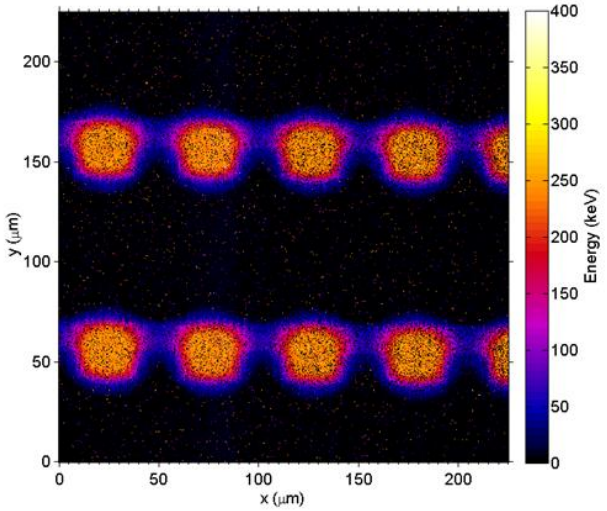

Fig. 5. Median energy map showing the spatial distribution of energy deposited by 2 MeV H^+ ions in the SVs of the even array. The detector was biased at -10 V. Odd array was not connected to readout electronics.

The charge collection enclosed by the yellow dashed line (square 1) has 100% CCE and corresponds to a 20 µm x 20 µm area surrounded by the n^+ ion implanted region with outer size of 30 µm x 30 µm (Figs. 1b and 6b). The region enclosed between square 1 and the white dashed line (square 2) corresponds to the region deposited by H^+ ions with energies between 170 keV and 200 keV, having slightly less than 100% CCE. This region corresponds to the n^+ implanted region of the 3D SV. Further reduction of CCE is seen in a 3 µm wide region of the SV between square 2 and the red dashed line (square 3). This is due to the combined effect of reduced electric field strength close to the boundary of the 3D SV (diffused charge collection) and partial energy deposition due to protons traversing the sides of the truncated pyramid of the 3D SV with a path length less than 10 µm. The total size of the charge collection image is approximately 30 µm x 30 µm, corresponding to the large base of the truncated square pyramid shape of the SV. The observed charge collection in the 3D SV corresponds to the etching pattern of silicon. Slight propagation of the diffused charge collection outside the geometrical dimensions of the square 3D SV along the Si bridge (pink tails) has been observed and is shown in Fig. 6b.

Although a large amount of silicon outside the SVs was etched away, charge produced by events occurring in the silicon bridge contributes slightly to the total charge collected in the 3D SV through lateral diffusion. Despite this, the amount of charge being collected outside the SV is low in comparison to previous generations of SOI planar microdosimeters [6, 7, 10], demonstrating that semi- 3D SVs are advantageous over traditional planar designs. Full etching of the surrounding silicon down to the silicon oxide layer of the SOI wafer is expected to fully remove events from outside the SVs. The truncated pyramid shape of the SV can be taken into account by calculating the average chord length through simulations used for microdosimetric spectra derivation.

b) Response of bridge microdosimeter to 5.5 MeV He^{2+}

The response of the bridge microdosimeter was further investigated using 5.5 MeV high LET He^{2+} ions. Fig. 7 shows MCA (Multi-channel analyzer) spectra and median energy

maps obtained from even array readout only. The microbeam was scanned across the microdosimeter using a scanning area of 0.9 mm x 0.9 mm. The microdosimeter was biased at 0 and -10 V. At 0 V the MCA energy spectrum did not show a clear peak due to the diffusion charge collection through the SVs, but at -10 V a 1400 keV peak was observed. This is in good agreement with the expected maximum value of 1480 keV from 5.5 MeV He^{2+} in 10 µm silicon and SiO_2 over-layer calculated by SRIM 2008. The SEM images presented in section A have demonstrated that the silicon surrounding the SVs was incompletely etched, leaving 5 µm of silicon active layer on the SOI device, leading to very low energy events in the energy spectrum.

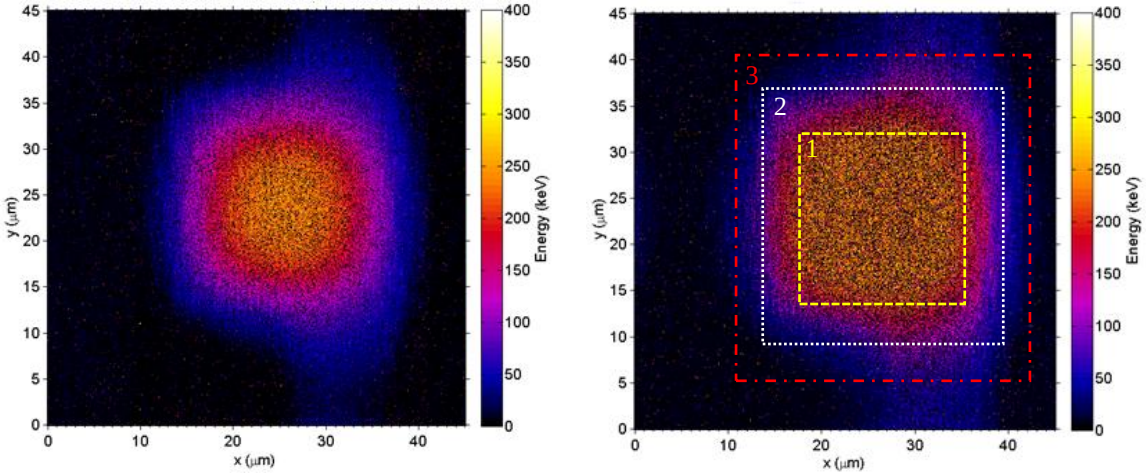

Fig. 6. Median energy map illustrating a single SV irradiated with a proton microbeam when biased at (a) 0 V and (b) -10V.

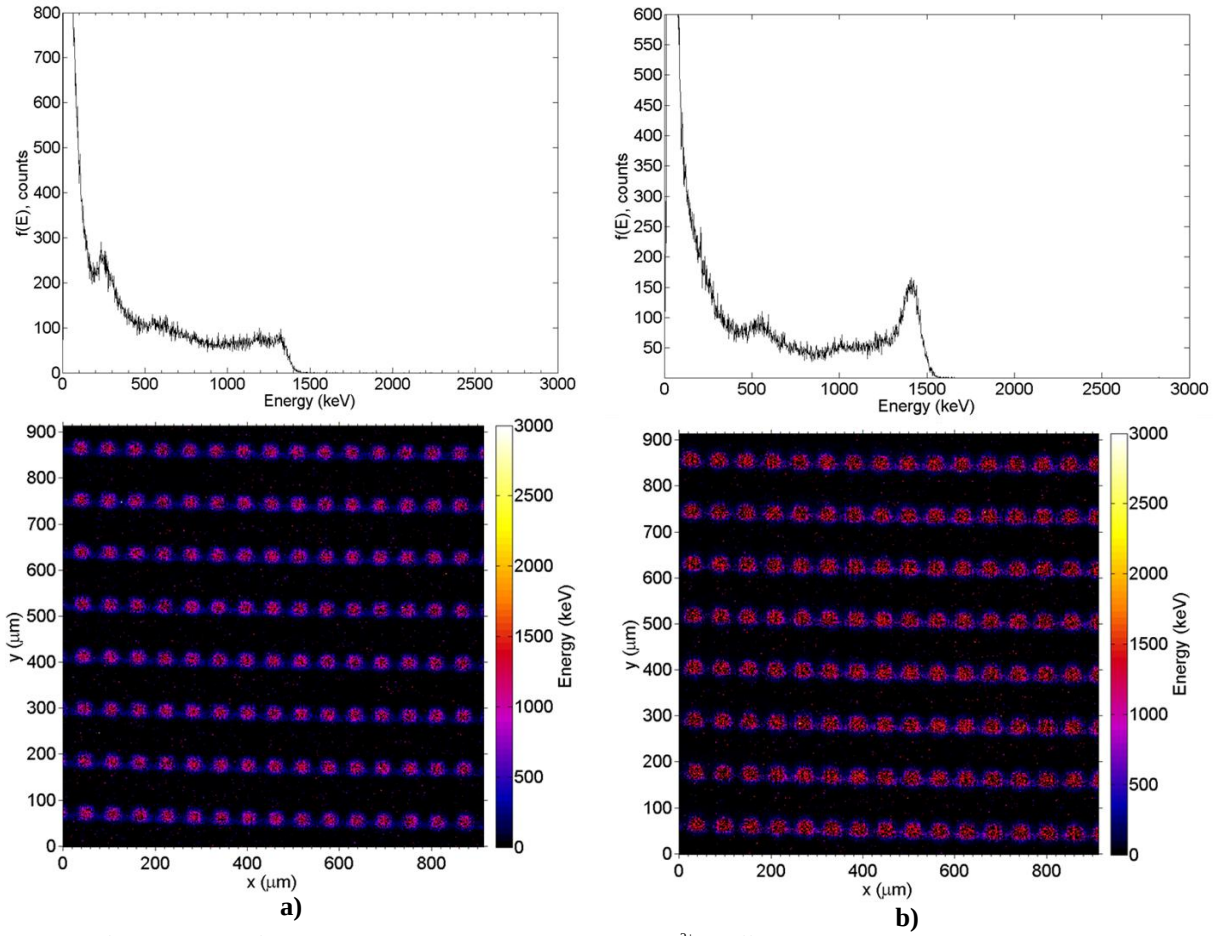

Fig. 7. Response of 3D even array of the mesa bridge microdosimeter to 5.5 MeV He^{2+} at different biases. (a) Energy spectrum and median energy map for 0V bias. (b) Energy spectrum and median energy map for -10V bias.

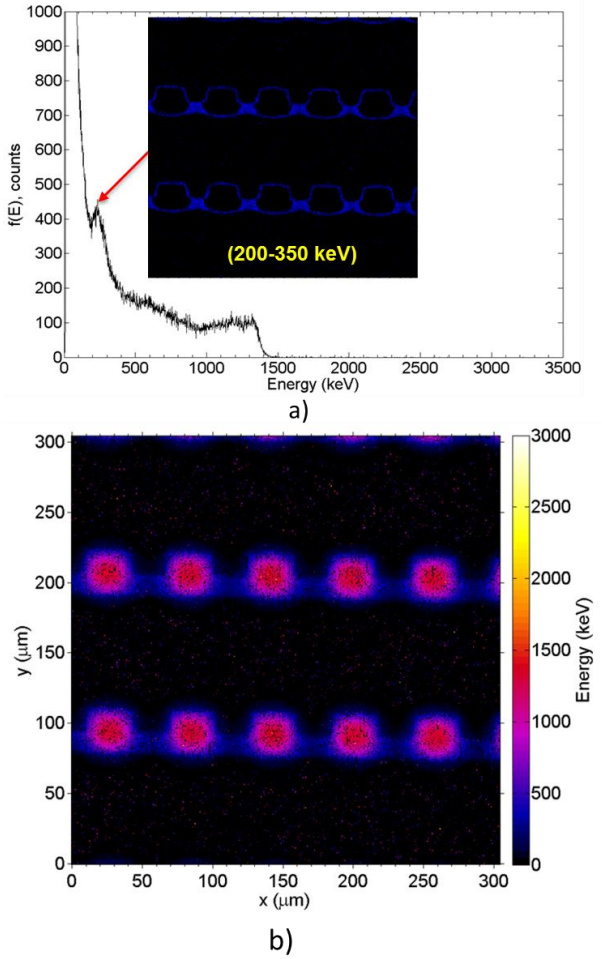

Fig. 8. Response of the 3D mesa bridge microdosimeter to 5.5 MeV He^{2+} at 0 V bias. (a) Energy spectrum with the median energy window comprising of events only in the lower energy peak indicated by the arrow (b) Median energy map. The data was obtained using scanning area of 0.3 mm x 0.3 mm.

A closer view of the charge collection in the device was obtained using a smaller scanning area of 0.3 mm x 0.3 mm (Fig. 8). The top image in Fig. 8 indicates that the peak seen at around 250 keV is mostly due to charge collection from the bridge region that connects the SVs.

Fig. 9 shows the response of the bridge microdosimeter when odd and even arrays were read out in parallel and both biased at -10V. All SVs are seen to be functioning and 100% yield is demonstrated.

Fig. 10 provides a closer view of the charge collection characteristics observed in the SVs. An approximately square SV shape was observed which is in good agreement with the design. Lower charge collection regions can be observed surrounding the SVs (purple color shown in the median energy map). This region is also related to boundaries of the truncated pyramid SVs which have shorter path lengths compared to when the particles are perpendicularly incident on the microdosimeter, as has been similarly observed with H ions.

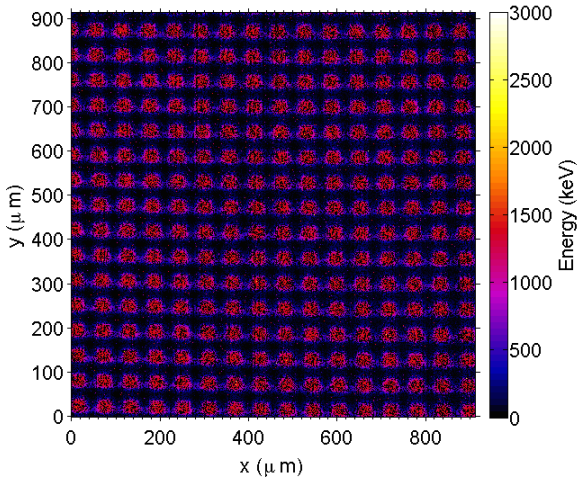

Fig. 9. Response of the microdosimeter at -10 V (odd and even arrays were connected in parallel). Scanning area is 0.9 x 0.9 mm^2.

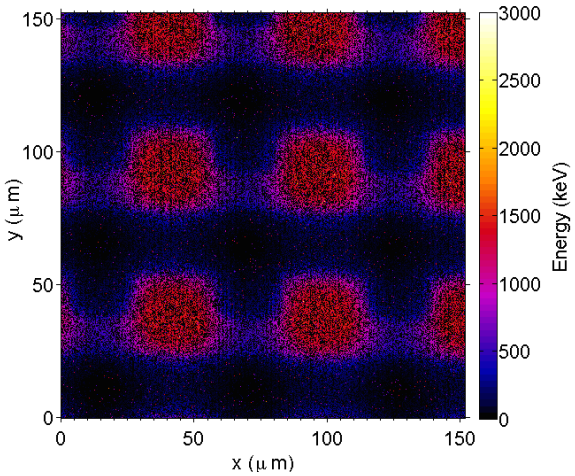

Fig. 10. Response of the microdosimeter at -10 V (odd and even arrays were connected in parallel). Scanning area is 150 x 150 μm^2.

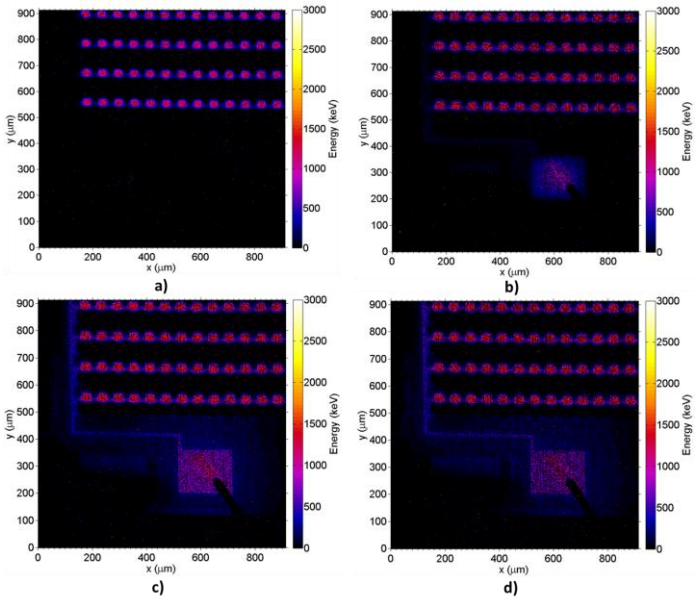

Fig. 11. Charge collection characteristics of the device near the bonding pad at (a) 0V, (b) -4V, (c) -6V and (d) -10V.

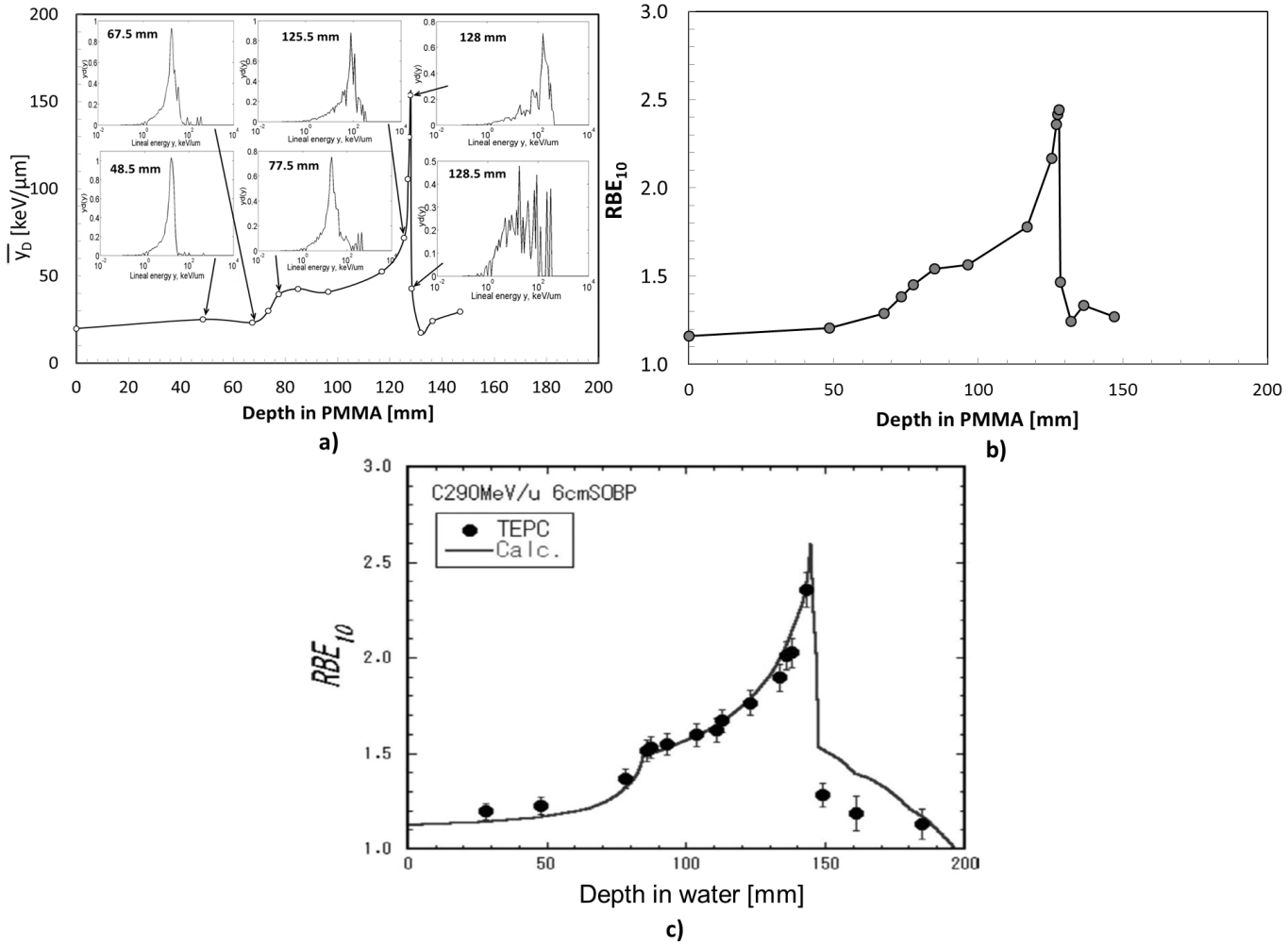

Fig. 12. (a) Dose-mean lineal energy deposition and microdosimetric spectra obtained along the SOBP, (b) derived RBE_{10} along the central axis of the ^{12}C ion beam, obtained by SOI bridge microdosimeter and (c) RBE_{10} distribution obtained by TEPC at NIRS [15]. Note: The phantom used in our experiment is PMMA while the TEPC measurements were carried out in water.

Fig. 11 shows charge collection under the Al tracks and bias pads connected to the p^+ cores of the SVs. At 0 V, no charge collection is observed in these regions, however at -4 V the charge starts collecting in the pad and extends along the aluminum track as the bias increases. This can be explained by the creation of an inversion layer under the oxide of the MOS capacitor, producing a thin depleted region. This effect can be eliminated by n^+ ion implantation under the oxide below the Al tracks and pad.

C. RBE_{10} study in ^{12}C ion beam

Using the bridge microdosimeter, microdosimetric spectra were obtained along the central axis of a ^{12}C SOBP for a 20 cm x 20 cm radiation field. The dose-mean lineal energy at each point of measurements was derived using the microdosimetric spectra and can be seen in Fig. 12a. The arrows in figure 12.a indicate positions along the SOBP where microdosimetric spectra were obtained. At 48.5 mm depth in the PMMA phantom, the microdosimetric spectrum is dominated by carbon ions crossing the detector and depositing lineal energies from 7 keV/µm to approximately 30 keV/µm, with the tail below 7 keV/µm corresponding to gamma radiation or to events in region with poor charge collection (e.g. minor diffusion charge collection from the "bridge" region close to the SV). At 67.5 mm depth in the PMMA phantom, a slight change in the shape of the microdosimetric spectrum can be observed due to slightly higher lineal energy deposition in the detector. This is due to the increased LET of ^{12}C ions and contribution of the fragments. At 77.5 mm a further contribution from the higher lineal energy events can be observed due to increasing LET of primary ^{12}C ions, especially due to the contribution from the distal part of the first partial pristine Brag Peak and fragments.

Derived RBE_{10} values based on the MKM and measured microdosimetric spectra with the bridge microdosimeter is presented in Fig. 12b. Derived RBE_{10} values match very well with those obtained from the TEPC measurements (Fig. 12c). Due to the high spatial resolution of the microdosimeter, more detailed RBE_{10} measurements were obtained at the end of the SOBP compared to the TEPC. The maximum derived RBE_{10} found using the bridge microdosimeter was approximately 2.6 which is in agreement with TEPC measurements. It should be noted that the bridge microdosimeter measurements were done in a PMMA phantom while TEPC measurements were carried out in water. The RBE_{10} in the fragmented part downstream of

the SOBP shows small bump that has not been observed from the measurements with TEPC (Fig 12c). The observed RBE_{10} peak can be explained by short range fragments and recoil C ions from the PMMA phantom that were absent in the water phantom when measurements were done with the TEPC. Additionally, an averaging effect due to the large size of the TEPC also contributed to these differences and demonstrates the advantage of high spatial resolution SOI microdosimeters.

IV. Conclusions

The CMRP 3D-mesa bridge microdosimeter was investigated in detail using scanning electron microscopy and 2 MeV H^+ and 5.5 MeV He^{2+} microbeams. The etching of silicon surrounding the SVs has shown to decrease low energy artefacts in comparison with planar SOI microdosimeters. However, due to the remaining un-etched silicon, some low energy events were still observed. Only minimal charge diffusion to the SVs was seen, mostly from the silicon bridge in close proximity to the SVs.

This work presented the first RBE_{10} derivation in a ^{12}C ion therapeutic beam using a high spatial resolution SOI microdosimeter. The obtained RBE_{10} values were found to be in good agreement with values obtained using a TEPC, with an exception at the distal part of the SOBP. This is due to TEPC measurements being carried out in water which lacks the C atoms in PMMA.

This presented bridge SOI microdosimeter is an intermediate step towards a fully 3D microdosimeter with free-standing 3D SVs microdosimeter. Future development of the silicon microdosimeters will include the fabrication of this 3D "mushroom" microdosimeter as well as an improved 3D mesa "bridge" microdosimeter. The improved 3D mesa bridge microdosimeter will be fully etched down to 10-µm depth and additionally, an n^+ stop layer will be ion implanted under the Al tracks and contact bias pads to eliminate charge collection below these regions at greater biases. Future work will also be focused on comparing the experimental response of the improved 3D bridge and 3D mushroom microdosimeters in a ^{12}C ion therapy beam with Geant4 simulations.

Acknowledgment

The authors would like to acknowledge the support of the Accelerator Operation Team, Institute of Environmental Research, Australian Nuclear Science and Technology Organization (ANSTO) for IBICC experiments and Professor Elena Pereloma and her team at the Australian Institute for Innovative Materials (AIIM), University of Wollongong for Scanning Electron Microscopy images.

References

[1] Rossi and M. Zaider, "Microdosimetry and its Applications," London: *Springer*, 1996.

[2] ICRU, "Microdosimetry," *ICRU Report 36*, 1983.

[3] P. D. Bradley, A. B. Rosenfeld, K. K. Lee, D. N. Jamieson, G. Heiser, and S. Satoh, "Charge collection and radiation hardness of a SOI microdosimeter for medical and space applications," *IEEE Trans. Nucl. Sci.*, vol. 45, no. 6, pp. 2700–2010, 1998.

[4] P. Bradley, "The development of a novel silicon microdosimeter for High LET radiation therapy," Ph.D. Thesis, University of Wollongong, Wollongong, Australia, 2000.

[5] I. M. Cornelius, A. B. Rosenfeld, R. Seigele, and D. Cohen, "LET dependence of the charge collection efficiency of silicon microdosimeters," *IEEE Trans. Nucl. Sci.*, vol. 50, no. 6, pp. 2373–2379, 2003.

[6] A. L. Ziebell, W. H. Lim, M. I. Reinhard, I. Cornelius, D. A. Prokopovich, R. Siegele, A. S. Dzurak, and A. B. Rosenfeld, "A cylindrical silicon-on-insulator microdosimeter: Charge collection characteristics," *IEEE Trans. Nucl. Sci.*, vol. 55, no. 6, pp. 3414–3420, 2008.

[7] J. Livingstone, D. A. Prokopovich, M. L. F. Lerch, M. I. Reinhard, M. Petasecca and A. B. Rosenfeld, "Large Area Silicon Microdosimeter for Dosimetry in High LET Space Radiation Fields: Charge Collection Study," *IEEE Trans. Nucl. Sci.*, vol. 59, no. 6, pp. 3126–3132, 2012.

[8] L. T. Tran, D. A. Prokopovich, M. Petasecca, M. L. F. Lerch, A. Kok, A. Summanwar, C. Da Via, M. I. Reinhard, K. Schjølberg-Henriksen and A. B. Rosenfeld, "3D Radiation Detectors: Charge Collection Characterisation and Applicability of Technology for Microdosimetry," *IEEE Trans. Nucl. Sci.*, vol. 61, no 4, pp. 1537–1543, 2014.

[9] L. T. Tran, S. Guatelli, M. L. F. Lerch, D. A. Prokopovich, M. I. Reinhard, J. F. Ziegler, M. Zaider and A. B. Rosenfeld, "A Novel Silicon Microdosimeter using 3D Sensitive Volume: Modeling the Response in Neutron Field Typical of Aviation," *IEEE Trans. Nucl. Sci.*, vol. 61, no. 4, pp. 1552–1557, 2014.

[10] W. H. Lim, A. L. Ziebell, I. Cornelius, M. I. Reinhard, D. A. Prokopovich, A. S. Dzurak, A. B. Rosenfeld, "Cylindrical silicon-on-insulator microdosimeter: Design, fabrication and TCAD modeling," *IEEE Trans. Nucl. Sci.*, vol. 56, no. 2, pp. 424–428, 2009.

[11] R. Siegele, D. Cohem, and N. Dytlewski, "The ANSTO high energy heavy ion microprobe," *Nucl. Instrum. Meth. Phys. Res. B*, vol. 158, pp. 31–38, 1999.

[12] J. F. Ziegler, J. P. Biersack and M. D. Ziegler, "SRIM – The Stopping and Range of Ions in Matter", *Ion Implantation Press*, 2008, Available: http://www.srim.org.

[13] Y. Kase, Y. Matsumoto, Y. Furusawa, H. Okamoto, T. Asaba, M. Sakama, H. Shinoda, "Microdosimetric measurements and estimation of human cell survival for heavy-ion beams," *Radiat. Res.*, vol. 166, no. 4, pp. 629–638, 2006.

[14] R. B. Hawkins, "A microdosimetric-kinetic model of cell death from exposure to ionizing radiation of any LET, with experimental and clinical applications," *International journal of radiation biology*, vol. 69, no. 6, pp. 739–739, 1996.

[15] Y. Kase; T. Kanai; M. Sakama; Y. Tameshige; T. Himukai; H. Nose; N. Matsufuji, "Microdosimetric Approach to NIRS-defined Biological Dose Measurement for Carbon-ion Treatment Beam," *Journal of Radiation Research*; ISSN: 0449-3060; vol. 52, no.1, pp. 59–68, 2011.

[16] P. D. Bradley and A. B. Rosenfeld, "Tissue equivalence correction for silicon microdosimetry detectors in boron neutron capture therapy," *Medical Physics*, vol. 25, no. 11, pp. 2220–2225, 1998.